

Old age increases microglial senescence, exacerbates secondary neuroinflammation, and worsens neurological outcomes after acute traumatic brain injury in mice



Rodney M. Ritzel¹, Sarah J. Doran¹, Ethan P. Glaser, Victoria E. Meadows, Alan I. Faden, Bogdan A. Stoica, David J. Loane*

Department of Anesthesiology and Center for Shock, Trauma and Anesthesiology Research (STAR), University of Maryland School of Medicine, Baltimore, MD, USA

ARTICLE INFO

Article history:

Received 19 September 2018
Received in revised form 31 January 2019
Accepted 9 February 2019
Available online 20 February 2019

Keywords:

Aging
Traumatic brain injury
Neuroinflammation
Microglia
Behavior

ABSTRACT

After traumatic brain injury (TBI), individuals aged over 65 years show increased mortality and worse functional outcomes compared with younger persons. As neuroinflammation is a key pathobiological mechanism of secondary injury after TBI, we examined how aging affects post-traumatic microglial responses and functional outcomes. Young (3-month-old) and aged (18-month-old) male C57Bl/6 mice were subjected to moderate-level controlled cortical impact or sham surgery, and neurological function was evaluated. At 72 hours after injury, brain, blood, and spleen leukocyte counts were assessed *ex vivo* using flow cytometry. Aged mice demonstrated more severe deficits in forelimb grip strength, balance and motor coordination, spontaneous locomotor activity, and anxiety-like behavior. These animals also exhibited more robust microglial proliferation and significantly higher numbers of brain-infiltrating leukocytes. Microglia in aged mice showed impairments in phagocytic activity and higher production of interleukin-1 β (IL-1 β). Infiltrating myeloid cells in aged TBI mice also had deficits in phagocytosis but showed diminished proinflammatory cytokine production and greater reactive oxygen species production. Expression of several senescence markers (Bcl-2, p16^{ink4a}, p21^{cip1a}, lipofuscin, and H2AX [pS139]) was increased with age and/or TBI in both microglia and injured cortex. Although there was no difference in the number of circulating blood neutrophils as a function of age, young mice exhibited more pronounced TBI-induced splenomegaly and splenic myeloid cell expansion. Thus, worse post-traumatic behavioral outcomes in aged animals are associated with exaggerated microglial responses, increased leukocyte invasion, and upregulation of senescence markers.

© 2019 Elsevier Inc. All rights reserved.

1. Introduction

Although the young adult population is most at risk for traumatic brain injury (TBI), a second peak incidence occurs in those aged 65 years and older (Flanagan et al., 2006). Older patients with TBI have increased mortality and worse functional outcomes compared with younger persons (Thompson et al., 2006). They show higher rates of intracerebral hemorrhage and poorer outcomes regardless of injury severity (Karibe et al., 2017; Papa et al., 2012; Susman et al., 2002). Falls at ground level are the most common mechanism of TBI in the elderly, responsible for more than 60% of such injuries (Filer and Harris, 2015). In fact, fall-related TBIs

have increased by 8% per year from 1998 to 2011 (Harvey and Close, 2012). Older patients with TBI have longer hospital stays and greater need for rehabilitation—highlighting the high morbidity, resource usage, and costs of managing this patient group (Coronado et al., 2005; Marin et al., 2017). These observations underscore the need to better understand how aging affects the pathogenesis of TBI.

Recent clinical and preclinical research studies have demonstrated the importance of the post-traumatic inflammatory response to subsequent neurodegeneration and related functional deficits (Faden et al., 2016; Simon et al., 2017). This inflammatory response is characterized by a stereotypic sequence of events involving the brain, its vasculature, and the peripheral immune system. Within minutes after TBI, tissue structure is disrupted, axons are stretched, and significant blood-brain barrier (BBB) breakdown occurs. Oxidative stress and release of proinflammatory mediators induce expression of adhesion molecules on brain

* Corresponding author at: Department of Anesthesiology, University of Maryland School of Medicine, 655 West Baltimore Street, #6-011, Baltimore, MD, 21201, USA. Tel.: +410-706-5188; fax: +410-706-1639.

E-mail address: dloane@som.umaryland.edu (D.J. Loane).

¹ Authors contributed equally to this work.

endothelial cells, promoting leukocyte entry into the brain (Abdul-Muneer et al., 2015). Microglia and infiltrating macrophages further amplify the immune response by secreting cytotoxic agents including cytokines (e.g., TNF, IL-1 β), reactive oxygen species (ROS), and extracellular proteases (e.g., MMP-9). Importantly, aging alone chronically alters microglial phenotype and sensitivity to injury-induced stimuli (Wong, 2013). Early studies had suggested that aging primes microglia so that they produce exaggerated levels of inflammatory mediators and that microglial responses to injury are generally amplified or dysregulated with age (Niraula et al., 2017). Because elderly TBI patients are believed to have poorer outcomes, they are often treated less aggressively (Gardner et al., 2018). However, recent data indicate that certain “younger elderly” people, aged 65–75 years, may have a comparable outcome to younger adults after mild-to-moderate TBI (Mak et al., 2012; Wan et al., 2016). These observations emphasize the need for more preclinical research to better understand age-related changes in TBI pathology and to develop age-specific targets for treatment.

Previous work has shown that the expression level of ionized calcium-binding adapter molecule 1 (Iba1), a microglia/macrophage marker, is chronically elevated in the hippocampus of aged mice after TBI (Sandhir et al., 2008). Furthermore, our laboratory demonstrated that aged mice have altered gene expression of proinflammatory and anti-inflammatory markers and increased numbers of reactive (bushy and hypertrophic) Iba1-positive microglia/macrophages in the cortex, hippocampus, and thalamus (Kumar et al., 2013). More recently, Morganti et al., 2016 reported that therapeutic targeting with a dual CCR2/5 antagonist significantly attenuated TBI-induced expression of inflammatory mediators and oxidative stress-related genes in aged mice. However, the understanding of cellular neuroimmune responses in the aged brain after TBI is very limited. Thus, we hypothesized that normal aging primes the microglial/macrophage response after TBI, resulting in an age-related exacerbation of post-traumatic neuroinflammation. In this study, we subjected young and aged mice to moderate-level controlled cortical impact (CCI) and evaluated functional outcomes using a battery of neurobehavioral tests and inflammatory responses using *ex vivo* analyses.

2. Methods and materials

2.1. Animals

Young adult (3-month-old) and aged (18-month-old) male C57BL/6 mice bred in-house obtained from the Jackson colony were housed on sawdust bedding in a specific pathogen-free facility (12 hours light/dark cycle). All animals had access to chow and water *ad libitum*. Animal procedures were performed in accordance with the NIH guidelines for the care and use of laboratory animals and approved by the Animal Care Committee of the University of Maryland School of Medicine.

2.2. Controlled cortical impact

Our custom-designed CCI injury device consists of a microprocessor-controlled pneumatic impactor with a 3.5-mm diameter tip as previously described (Loane et al., 2009). Briefly, mice were anesthetized with isoflurane evaporated in a gas mixture containing 70% N₂O and 30% O₂ and administered through a nose mask. Mice were placed on a heated pad, and core body temperature was maintained at 37 °C. The head was mounted in a stereotaxic frame, a 10-mm midline incision was made over the skull, and the skin and fascia were reflected. A 5-mm craniotomy was made on the central aspect of the left parietal bone. The impounder tip of the injury device was then extended to its full stroke distance

(44 mm), positioned to the surface of the exposed dura, and reset to impact the cortical surface. Moderate-level CCI was induced using an impactor velocity of 6 m/s, deformation depth of 1 mm, and a dwell time of 50 ms (Loane et al., 2009). After injury, the incision was closed with interrupted 6–0 silk sutures, anesthesia was terminated, and the animal was placed into a heated cage to maintain normal core temperature for 45 minutes after injury. Sham animals underwent the same procedure as CCI mice except for craniotomy and cortical impact.

2.3. Open field analysis

The open field test was used to measure locomotor activity on postinjury day 2 as previously described (Zhao et al., 2012). The apparatus consists of an open field (22.5 cm \times 22.5 cm) with 2 adjacently located imaginary circular zones. Mice were individually placed in a corner facing the wall of the open-field chamber and allowed to freely explore the chamber for 5 minutes. The distance traveled was recorded by the ANY-Maze software (Stoelting Co, Wood Dale, IL, USA). Mice were baseline tested before CCI and on postinjury day 2.

2.4. Rotarod

Motor function was assessed using a rotarod as previously described (Doran et al., 2018). Before sham or CCI, all animals were trained 3 trials per day for 2 consecutive days on the rotarod apparatus (IITC, Inc, Life Sciences, St. Petersburg, FL, USA). Latency was assessed by measuring the length of time each mouse remained on the rotating drum as it accelerated from 4 to 40 rpm over a span of 2 minutes. The latency of each mouse to fall from the rotating drum was recorded for each trial (in seconds), and the average latency was used for further analysis. Animals were then tested on day 1, 2, and 3 after injury, with 3 trials as in the training period, and the average latency was recorded.

2.5. Grip strength

Grip strength was measured using a digital grip strength meter (Bioseb BP, In Vivo Research Instruments, France) on day 1, 2, and 3 after injury, as previously described (Jacotte-Simancas et al., 2015). Forelimb grip strength was measured from the mouse using both the ipsilateral and contralateral forepaws together. The mouse was held by its tail, the forelimbs were placed on the grasping metal wire grid, and the mouse gripped the wire grid attached to the force transducer. Once the grip was secured, the animal was slowly pulled away from the bar. The maximal average force exerted on the grip strength meter by both forepaws was averaged from 3 trials per day for each mouse, for 2 consecutive days.

2.6. Cylinder test

The cylinder test was used to assess asymmetry in forelimb usage as described previously (Venna et al., 2012). Each animal was individually placed in a transparent plexiglass cylinder of 9 cm diameter and 15 cm height during the test. Forelimb use of the first contact against the cylinder wall after rearing and during lateral exploration was analyzed using the following criteria: a total of 20 limb placements on the cylinder wall were recorded during the 10 minute session. A mirror was placed behind the cylinder with an angle to enable the rater to view forelimb movements when the mouse was turned to other side. The final score = (nonimpaired forelimb use [right] – impaired forelimb use [left]) / (nonimpaired forelimb use + impaired forelimb use + both limbs movement). Mice were assessed before CCI and on day 2 after injury. Of the

19 mice in each group that were tested, 32% of young mice ($N = 6$) and 36% of aged mice ($N = 7$) did not perform and were excluded from the analysis.

2.7. Flow cytometry

Body weights were recorded, and immediately after mice were euthanized, blood (200 μ L) was drawn by cardiac puncture with heparinized needles. After transcardial perfusion with 60 mL of ice-cold sterile PBS, the spleen was removed, weighed, and processed by mechanical disruption on a 70- μ m filter screen. Red blood cell lysis was achieved by successive 10-minute incubations with Tris-ammonium chloride (Stem Cell Technologies, Vancouver, Canada). Splenocytes were subsequently washed and resuspended in a total of 5 mL of RPMI (Lonza Group, Basel, Switzerland) from which 500 μ L was then transferred into FACS tubes. Brain hemispheres were mechanically digested using a razor blade to mince tissue and were passed through a 70- μ m filter using RPMI. Central nervous system (CNS) tissue was then enzymatically digested using DNase (10 mg/mL; Roche, Mannheim, Germany), collagenase/dispase (1 mg/mL; Roche), and papain (25 U; Worthington Biochemical, Lakewood, NJ, USA) for 1 hour at 37 °C in a shaking CO₂ incubator (200 rpm). Tissue homogenates were centrifuged at 1500 rpm for 5 minutes at 4 °C. The supernatant was discarded, and the cells were resuspended in 70% Percoll (GE Healthcare, Pittsburgh, PA, USA) and underlaid in 30% Percoll. This gradient was centrifuged at 500 g for 20 minutes at 21 °C. Myelin was removed by suction, and cells at the interface were collected. Leukocytes were washed and blocked with mouse Fc Block (eBioscience, San Diego, CA, USA; clone 93) before staining with primary antibody-conjugated fluorophores (CD45-eF450 [30-F11], CD11b-APCeF780 [M1/70], Ly6C-APC [HK1.4], and Ly6G-PE [1A8] purchased from eBioscience, whereas CD45-PerCP-Cy5.5 [30-F11] and CD11b-PerCP-Cy5.5 [M/70] purchased from Biolegend, San Diego, CA, USA). For live/dead cell discrimination, a fixable viability dye, Zombie Aqua (Biolegend), was dissolved in DMSO according to the manufacturer's instructions and added to cells in a final concentration of 1:200. Data were acquired on an LSRII using FACSDiva 6.0 (BD Biosciences, San Jose, CA, USA) and analyzed using FlowJo (Tree Star, San Carlos, CA, USA). A standardized gating strategy was used to identify microglia (CD45^{int}CD11b⁺Ly6C⁻) and brain-infiltrating myeloid cells (CD45^{hi}CD11b⁺), including monocyte (CD45^{hi}CD11b⁺Ly6C⁺Ly6G⁻) and neutrophil (CD45^{hi}CD11b⁺Ly6C⁺Ly6G⁺) populations as previously described (Ritzel et al., 2018b). Cell-specific fluorescence-minus-one (FMO) controls were used to determine the positivity of each antibody. Cell count estimations were performed using the CountBright absolute counting beads (40 μ L/test; Invitrogen, Carlsbad, CA, USA) according to the manufacturer's instructions.

For intracellular cytokine staining, leukocytes were collected as described previously, and 1 μ L of GolgiPlug containing brefeldin A (BD Biosciences) was added to 500 μ L complete RPMI. Cells were then resuspended in Fc Block, stained for surface antigens, and washed in 100 μ L of fixation/permeabilization solution (BD Biosciences) for 20 minutes. Cells were washed twice in 500 μ L permeabilization/wash buffer (BD Biosciences) and resuspended in an intracellular antibody cocktail containing cytokine antibodies (MMP-9-R-PE, StressMarq Biosciences [SMC-396D]; p16^{ink4a}-APC, StressMarq Biosciences [SPC-1280D]; p21^{cip1}-FITC, StressMarq Biosciences [SPC-1281]; H2AX pS139-PE, MACS Miltenyi Biotec [130-107-585]; NOX2-AF647, Bioss Antibodies [bs-3889R]; TNF-PE-Cy7, eBioscience [MP6-XT22]; IL-1 β -PerCP-eF710, eBioscience [NJTEN3]; and Bcl-2-PE-Cy7, BioLegend [BCL/10C4]) and fixed.

For detection of ROS, leukocytes were incubated with dihydro-rhodamine (DHR) 123 (5 mM; 1:500 in RPMI; Ex/Em: 500/536), a cell-permeable fluorogenic probe (Life Technologies/Invitrogen, Carlsbad, CA, USA). Cells were loaded for 20 minutes at 37 °C,

washed 3 times with FACS buffer (without NaAz) and then stained for surface markers including viability stain.

Phagocytic activity of myeloid cells was performed as described (Ritzel et al., 2015a) with minor modification. Briefly, red fluorescent carboxylate-modified polystyrene latex beads (0.5 μ m mean diameter; Sigma) were added to freshly isolated cells in a final dilution of 1:100 (in RPMI). After 45 minutes of incubation at 37 °C, the cells were washed twice, resuspended in FACS buffer, stained for surface markers, and fixed in paraformaldehyde.

2.8. RNA isolation and qPCR analysis

Total RNA was extracted from the ipsilateral cortex of young and aged sham and CCI mice using an RNeasy Mini kit (Qiagen, Valencia, CA, USA) with on-column DNase treatment (Qiagen). cDNA was then made using a VERSO cDNA Reverse Transcription kit (Thermo Scientific, Pittsburgh, PA, USA). Real-time quantitative PCR analysis for target mRNAs was performed using TaqMan gene expression assays (GAPDH, Mm99999915_g1; p16^{ink4a} Mm00494449_m1; and p21^{cip1} Mm04205640_g1). Samples were assayed in triplicate in one run (40 cycles), which was composed of 3 stages, 50 °C for 2 minutes, 95 °C for 10 seconds for each cycle (denaturation) and finally the transcription step at 60 °C for 1 minute. Gene expression was normalized by GAPDH per sample and then compared with the control sample (young sham) to determine relative expression values by the 2- $\Delta\Delta$ Ct method.

2.9. Protein isolation and Western blot analysis

Proteins from ipsilateral cortical tissue of young and aged mice were extracted using RIPA buffer, equalized, and loaded onto 5%–20% gradient gels for SDS PAGE (Bio-Rad; Hercules, CA, USA). Proteins were transferred onto nitrocellulose membranes using a dry transfer method and then blocked for 1 hour in 5% milk in 1 \times TBS containing 0.05% Tween-20 (TBS-T) at room temperature. The membrane was incubated in rabbit Anti-CDKN2A/p16^{ink4a} antibody [EPR20418] (ab211542) (1:1000; Abcam, Cambridge, UK), rabbit Anti-p21^{cip1} antibody [EPR18021] (ab188224) (1:1000; Abcam), or mouse anti- β -Actin (1:5000; Sigma-Aldrich) overnight at 4 °C, then washed 3 times in TBS-T, and incubated in appropriate HRP-conjugated secondary antibodies (Jackson ImmunoResearch Laboratories, West Grove, PA, USA) for 2 hours at room temperature. Membranes were washed 3 times in TBS-T, and proteins were visualized using SuperSignal West Dura Extended Duration Substrate (Thermo Scientific, Rockford, IL, USA). Chemiluminescence was captured using ChemiDoc XRS+ System (Bio-Rad), and protein bands were quantified by densitometric analysis using BioRad Molecular Imaging software. The data presented reflect the intensity of target protein band normalized based on the intensity of the endogenous control for each sample (expressed in arbitrary units).

2.10. Statistical analyses

Data from individual experiments are presented as mean \pm SEM. Group effects were determined by the two-way analysis of variance (ANOVA) with Sidak or Tukey post hoc correction for multiple comparisons. For all behavioral and flow cytometry experiments, $N = 7$ for sham and $N = 12$ for CCI mice per age group were used. A separate cohort of $N = 4$ sham and $N = 6$ CCI mice per age group were used to perform all gene and protein analyses. Behavioral data were also analyzed by the two-way repeated-measures ANOVA. All behavioral and ex vivo studies were performed by an investigator blinded to surgical condition. Statistical analysis was performed

using the GraphPad Prism software v. 6.0 (GraphPad Software, Inc, La Jolla, CA, USA); $p < 0.05$ was considered statistically significant.

3. Results

3.1. Aging worsens functional outcomes after acute TBI

We induced moderate-level CCI in young adult (3-month-old) and aged (18-month-old) male C57Bl/6 mice and evaluated neurological function daily across the first 72 hours after injury using a battery of behavioral tests to determine the extent of TBI-induced deficits in locomotor activity, motor coordination, grip strength, and contralateral forelimb impairment. We observed that the percent of body weight loss was initially higher in young TBI mice at day 1 after injury but subsequently returned to baseline weight by day 2 (Fig. 1A). In contrast, aged TBI mice exhibited a gradual but continued increase in body weight loss up to day 3 after

injury compared with baseline, age-matched sham and young TBI mice.

Motor performance was evaluated using an accelerating rotarod. As previously reported (Shoji et al., 2016), normal aging significantly decreased the latency to fall at baseline. After CCI, both groups spent less time on the rotarod relative to baseline (Fig. 1B). TBI-induced motor function deficits in young mice reached their maximum at the same latency to fall time observed in aged sham mice, whereas aged TBI mice spent significantly less time on the rotarod than age-matched controls. Recovery during this acute period appeared to favor aged mice, with young TBI mice exhibiting continued impairment in motor function by day 3 after injury, whereas aged TBI mice had similar fall latencies as age-matched sham mice at this time point. We then measured grip strength using a handheld device. Consistent with other studies (Ge et al., 2016), normal aging resulted in a decrease in grip strength, whereas TBI caused significant impairment in forelimb grip force in both young and aged mice (Fig. 1C). Deficits in grip strength reached

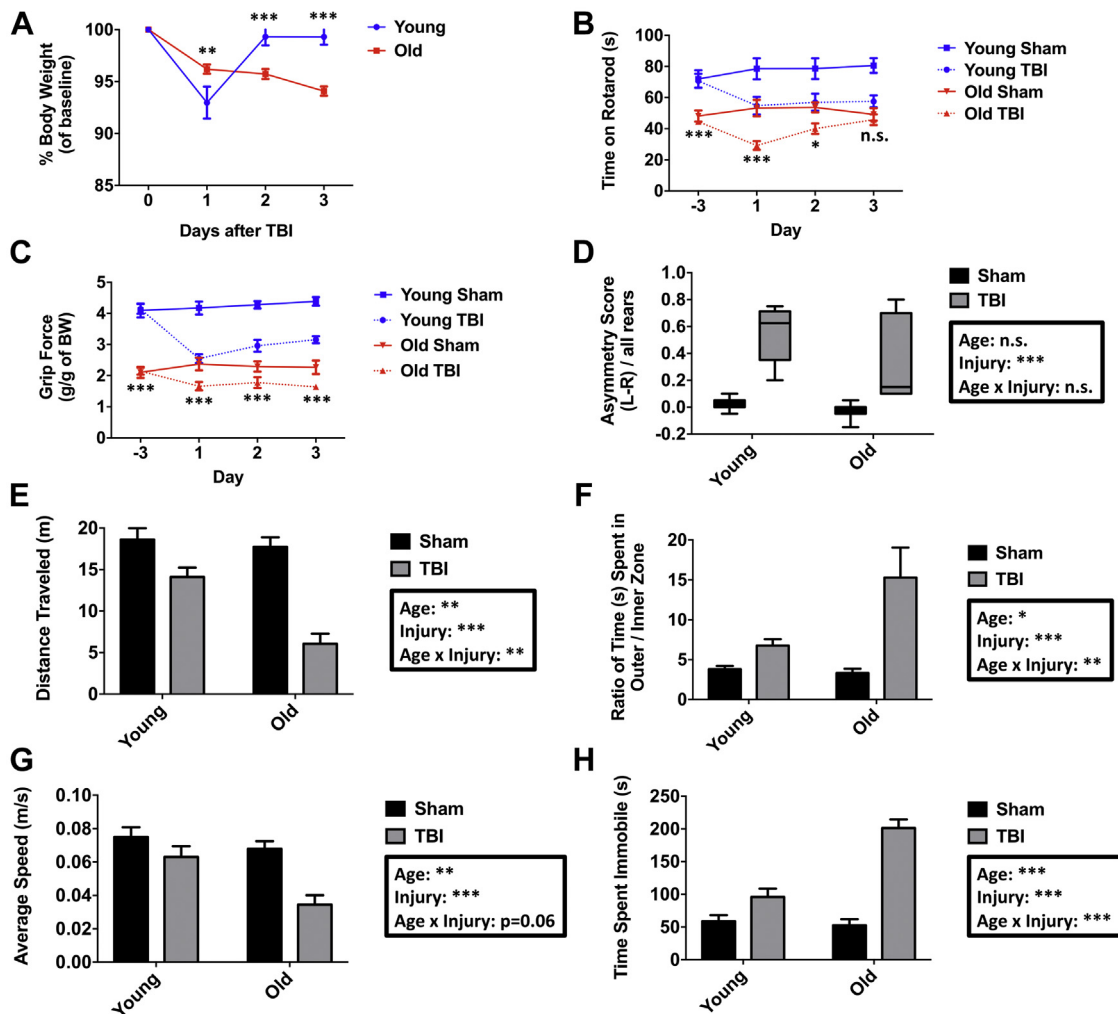


Fig. 1. Age-related differences in acute behavioral deficits after TBI. The percent change in body weight from baseline was recorded for young and aged mice for 3 days after injury (A). Time spent on an accelerating rotarod was evaluated over the course of 3 days after TBI (B). Grip strength for young and old mice in sham and TBI groups is shown (C). Cylinder testing demonstrated significant asymmetric forelimb use in both age groups after TBI (D). Animals were then evaluated in an open-field apparatus at 3 days after TBI to measure spontaneous locomotor activity. The total distance traveled in the open-field apparatus for sham and TBI mice is shown (E). The ratio of the total time spent in the inner versus outer zones of the open field demonstrated significant effects of age and injury (F). The average speed (G) and time spent immobile (H) in the open field showed a robust interaction between age and injury. For all experiments, $N = 7$ sham and $N = 12$ TBI/group. Statistical comparisons between groups were determined by the one- or two-way repeated-measures ANOVA with Tukey's multiple comparisons test. For cylinder and open-field analysis, the analysis was performed using the two-way ANOVA with Tukey's test. Significant group effects of age, injury, and interaction between age and injury are shown in each box. Error bars show mean \pm SEM. * $p < 0.05$, ** $p < 0.01$, and *** $p < 0.001$. Abbreviations: ANOVA, analysis of variance; BW, body weight; g, gram; L, left; m, meters; n.s., not significant; R, right; s, seconds; SEM, standard error of mean; TBI, traumatic brain injury.

their lowest point in young TBI mice at levels that were similar to aged sham mice. Although the change in grip strength was not as pronounced in aged mice after TBI relative to young mice, the absolute grip force was significantly lower than both age-matched sham control and the young TBI group. Neither young nor aged TBI groups showed a complete restoration in grip strength during this acute time period. We then assessed for unilateral forelimb impairment using the cylinder test. TBI induced spontaneous forelimb-use asymmetry in both young and aged mice at 3 days after injury, with greater preference for using the unimpaired right forepaw (Fig. 1D). Although these changes were robust, age-related deficits in sensorimotor function could not be determined given the high incidence of mice unable to perform this task (32% of young TBI mice and 36% of aged TBI mice).

We also measured locomotor activity. Open field testing at 48 hours after injury revealed a significant effect of TBI on spontaneous locomotor activity, with aged TBI mice traveling comparatively shorter distances than their younger counterparts (Fig. 1E). Although both groups spent more time along the perimeter in the outer zone of the maze, aged TBI mice spent comparably less time in the inner zone, indicating that aging modified TBI-induced anxiety-like behaviors (Fig. 1F). Despite spending more time in the outer zone after TBI, the average speed and time spent immobile was significantly decreased and increased, respectively, in an age-dependent manner (Fig. 1G and H). These data indicate that TBI causes an age-related worsening of locomotor impairment, evidenced by less activity and slower movements. Aged TBI mice also showed a greater preference for the edges of the open field, indicating a more pronounced anxiety-driven aversion to being in open areas of the maze. Taken together, our findings demonstrate an important interaction between age and TBI that result in an age-related worsening of motor coordination and muscle strength.

3.2. Aging alters microglial sensitivity to TBI and increases neutrophil infiltration

Inflammation is a key driver of TBI (Simon et al., 2017). To better understand the cellular correlates of the observed age-related worsening in neurological outcomes, we next evaluated the inflammatory response in the brain using flow cytometry (Fig. 2A). The absolute number of living CD45^{int}CD11b⁺Ly6C⁻ microglia was lower in aged brains (Fig. 2B). Despite these baseline differences, TBI caused a significant increase in microglia counts in both age groups, with old mice displaying relatively more robust proliferation than their younger counterparts. Relative to each sham group, however, significantly greater rates of microglia proliferation were seen in old mice with respect to their younger counterparts (Fig. 2C; 1.45 ± 0.1-fold increase in young TBI versus 2.11 ± 0.2-fold increase in aged TBI). Next, we examined whether aging makes the brain more vulnerable to peripheral leukocyte invasion after TBI. The total number of infiltrating CD45^{hi} leukocytes was dramatically increased in both young and aged TBI mice; however, aged TBI mice showed significantly greater numbers of peripheral immune cells than young (Fig. 2D). The vast majority of these cells were of myeloid origin (CD45^{hi}CD11b⁺), whereas bulk lymphocyte (CD45^{hi}CD11b⁻) infiltration was largely negligible at this acute time point. Compositional analysis of the infiltrating myeloid population revealed an age-related change in the relative proportion of Ly6C⁺Ly6G⁺ neutrophils and Ly6C⁺Ly6G⁻ monocyte derivatives, in that, aging increased the frequency of neutrophil extravasation in the TBI brain (Fig. 2E). These findings suggest that aging alters the proliferative sensitivity of microglia and makes the brain more permeable to leukocyte invasion after TBI, with aged TBI mice showing a greater bias toward neutrophil recruitment.

3.3. Microglial and infiltrating myeloid cell responses to TBI are functionally distinct and altered with age

Neuroinflammation is characterized by changes in microglia/macrophage activation that lead to increased ROS generation, proinflammatory cytokine production, and phagocytic activity. We addressed these changes using an ex vivo flow cytometry approach. Oxidative stress was measured using NOX2 (NADPH oxidase 2) protein expression and dihydrorhodamine 123, a fluorogenic probe used to detect ROS, such as peroxide and peroxynitrite. A significant interaction between age and TBI was found for NOX2 expression and ROS production in microglia, as reflected by higher ROS levels in aged microglia and after TBI (Fig. 3A and C). Infiltrating myeloid cells showed greater NOX2 and ROS production relative to resident microglia (813 ± 27 vs. 1550 ± 26; $p < 0.001$ and 4399 ± 224 vs. 6845 ± 394; $p < 0.01$, respectively). Interestingly, infiltrating myeloid cells in the aged brain displayed less NOX2 expression and higher ROS production than those found in young TBI brains (Fig. 3B and D), suggesting that NOX2 activity rather than its expression per se may be accelerated with age.

Debris clearance and removal of apoptotic neurons is a critical function of microglia/macrophages after acute brain injury (Simon et al., 2017). Therefore, we assessed phagocytic activity in leukocytes isolated from the TBI brain using a bead-engulfment assay. Microglial phagocytic activity was significantly increased after TBI in young and aged mice but was significantly impaired in aged microglia (Fig. 3E). Infiltrating myeloid cells were comparably better at engulfing beads than resident microglia (29,133 ± 1369 vs. 38,550 ± 889; $p < 0.001$); however, engulfment was significantly impaired in both resident microglia and infiltrating myeloid cells in the aged TBI brain (Fig. 3F). These data indicate that debris clearance mechanisms such as the phagocytic removal of damaged cells may be highly impaired in old immune cells.

To further analyze the connection between aging and TBI-induced neuroinflammation, we examined protein production of inflammation-related molecules, including tumor necrosis factor (TNF), interleukin-1 beta (IL-1 β), and matrix metalloproteinase-9 (MMP-9). MMP-9 expression and activity are upregulated acutely after TBI and are involved in the degradation of the extracellular matrix, resulting in endothelial dysfunction and BBB permeability (Zhang et al., 2016). Our data demonstrate that microglial MMP-9 production is significantly increased after TBI (Fig. 3G). The mean fluorescence intensity of MMP-9 was diminished in infiltrating myeloid cells with age after TBI (Fig. 3H). We next examined the production of the proapoptotic cytokine, TNF. There was a significant interaction of age for microglial TNF production, with aged microglia showing relatively higher TNF levels than young microglia (Fig. 3I). Similarly, a significant interaction of TBI for microglial TNF production was observed; however, the interaction between age and TBI was not significant. Infiltrating myeloid cells produced similar levels of TNF relative to resident microglia; however, aging was associated with significantly lower expression in these cells (Fig. 3J). IL-1 β is a byproduct of inflammasome signaling that is involved in a variety of cellular activities, including cell proliferation, differentiation, and apoptosis. IL-1 β also plays a key role in aging and disease (Goldberg and Dixit, 2015). Microglial production of IL-1 β was significantly increased with both age and after TBI, although the interaction between age and TBI was not significant (Fig. 3K). Young microglia produced higher levels of IL-1 β after TBI but did not exceed the levels detected in aged sham microglia. Notably, infiltrating myeloid cells were the predominant IL-1 β producers in the TBI brain (2890 ± 102 vs. 7369 ± 611; $p < 0.001$), whereas myeloid IL-1 β production was significantly diminished with age (Fig. 3L). Our data indicate that both resident microglia and infiltrating myeloid cells are important contributors of

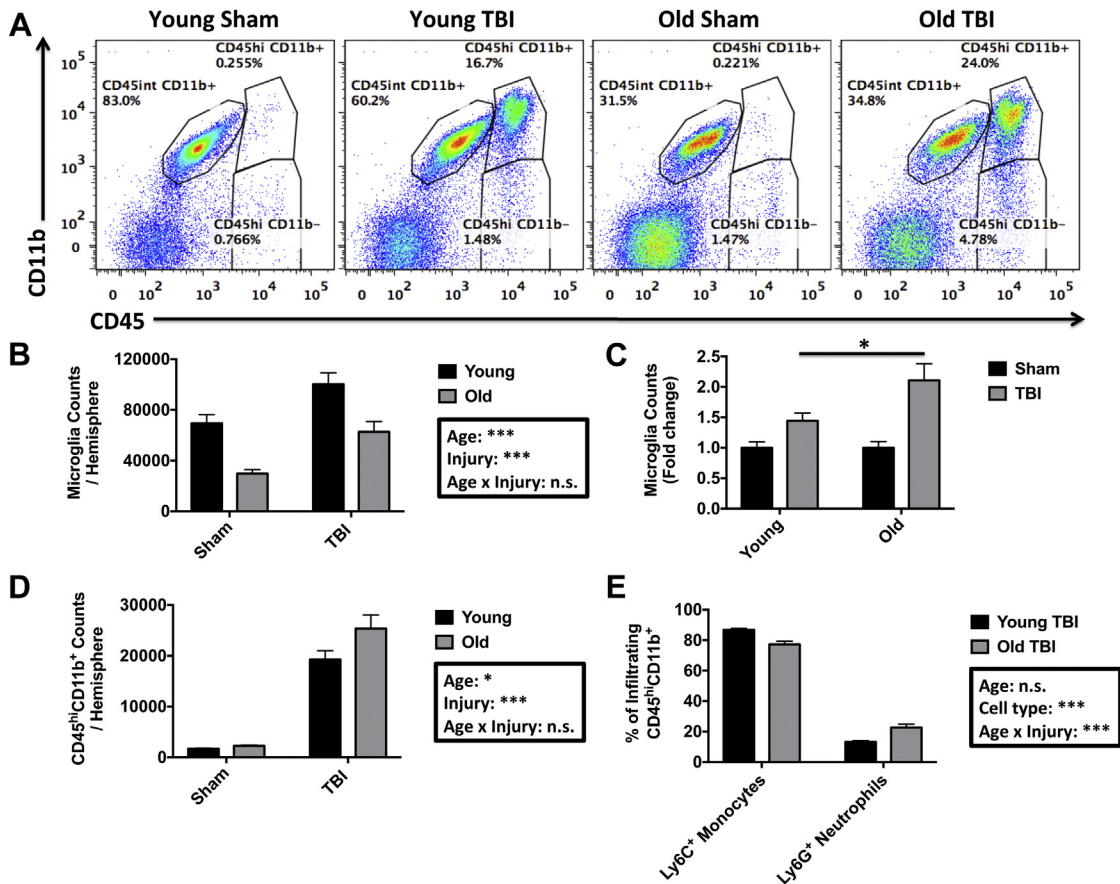


Fig. 2. Old age alters the microglial proliferation response and leukocyte extravasation after TBI. Representative dot plots show the identification of CD45^{int} microglia and CD45^{hi} infiltrating peripheral myeloid cells in the sham-injured and TBI brain of young and old mice at day 3 after surgery (A). The absolute number of microglia per ipsilateral hemisphere was determined and shows a significant decrease in microglia number at baseline in old mice (B). Microglia counts expressed as a fold-change relative to each sham group demonstrated a greater TBI-induced microglial proliferative response in old mice (C). The number of brain-infiltrating myeloid cells is shown for young and old mice after injury (D). The relative composition of these CD45^{hi} myeloid cells reveals a modest but significant neutrophilic shift in old mice after TBI (E). For all experiments, N = 7 sham and N = 12 TBI/group. Statistical comparisons between groups were determined by the two-way ANOVA with Tukey's multiple comparisons test. Significant group effects of age, injury, and interaction between age and injury are shown in each box. Error bars show mean \pm SEM. * $p < 0.05$, and *** $p < 0.001$. Abbreviations: ANOVA, analysis of variance; n.s., not significant; SEM, standard error of mean; TBI, traumatic brain injury.

proinflammatory response after TBI. Notably, aging blunted the production of TNF and IL-1 β in the infiltrating myeloid population, highlighting the important age-related alterations in the regulation of cytokine signaling pathways after TBI.

3.4. Microglial expression of senescence markers is increased with age and acutely after TBI

Aging is associated with an increase in inflammatory signaling, cellular dysfunction, and senescence (Fulop et al., 2017). Although relatively low in number, senescent macrophages are believed to be significant contributors of inflamm-aging, a phenomenon characterized by an age-related elevation in chronic, low-grade inflammation (Prattichizzo et al., 2016). To date, few studies have confirmed the expression of senescence markers (e.g., p-H2AX, BCL-2, p16^{ink4a}, and p21^{cip1a}) in the aged microglia population, or after TBI. First, we observed that the relative size and granularity (i.e., forward scatter [FSC] and side scatter [SSC], respectively) of microglia after TBI was significantly increased in both young and aged groups, with young TBI mice exhibiting a greater change from age-matched sham levels in these parameters (Fig. 4A and B). The size and granularity of microglia in young TBI mice was significantly less than that observed with normal aging. Aging also results in increased lipofuscin accumulation in microglia that localize to lysosomal inclusions and may reflect impairment in autophagy

function (Marschallinger et al., 2017; von Bernhardt et al., 2015). We found that microglial autofluorescence in the empty fluorescein isothiocyanate (FITC) or phycoerythrin (PE) channels was more than doubled with normal aging (Fig. 4C and D). TBI induced a significant increase in microglial autofluorescence in young TBI mice, but these levels did not exceed those of either the aged sham or TBI groups. At the protein level, our analysis reveals that 2 additional markers of senescence, the anti-apoptotic protein Bcl-2 (Hernandez-Segura et al., 2018), and histone H2AX phosphorylation (pS139), indicative of double-stranded DNA breaks (Rogakou et al., 1998), were significantly increased in microglia with both age and TBI (Fig. 4E and F). However, the interaction between age and TBI was not significant for these senescence markers.

Finally, we examined for the upregulation of the cellular senescence markers, p16^{ink4a} and p21^{cip1a}, tumor suppressor proteins involved in cell cycle arrest (Childs et al., 2014; Herranz and Gil, 2018). Gene and protein expressions were measured in cortical tissue and in microglia. A significant interaction between age and TBI was demonstrated for p16^{ink4a} gene expression in the cortex, wherein TBI induced nearly two-fold higher expression in the aged injured than young injured cortex (Fig. 5A). There was a significant increase in p21^{cip1a} transcription after TBI in both young and aged cortices (Fig. 5B), but there was no interaction between age and TBI. Consistently, TBI also significantly increased the relative protein expression of both p16^{ink4a} and p21^{cip1a} in the cortex, as

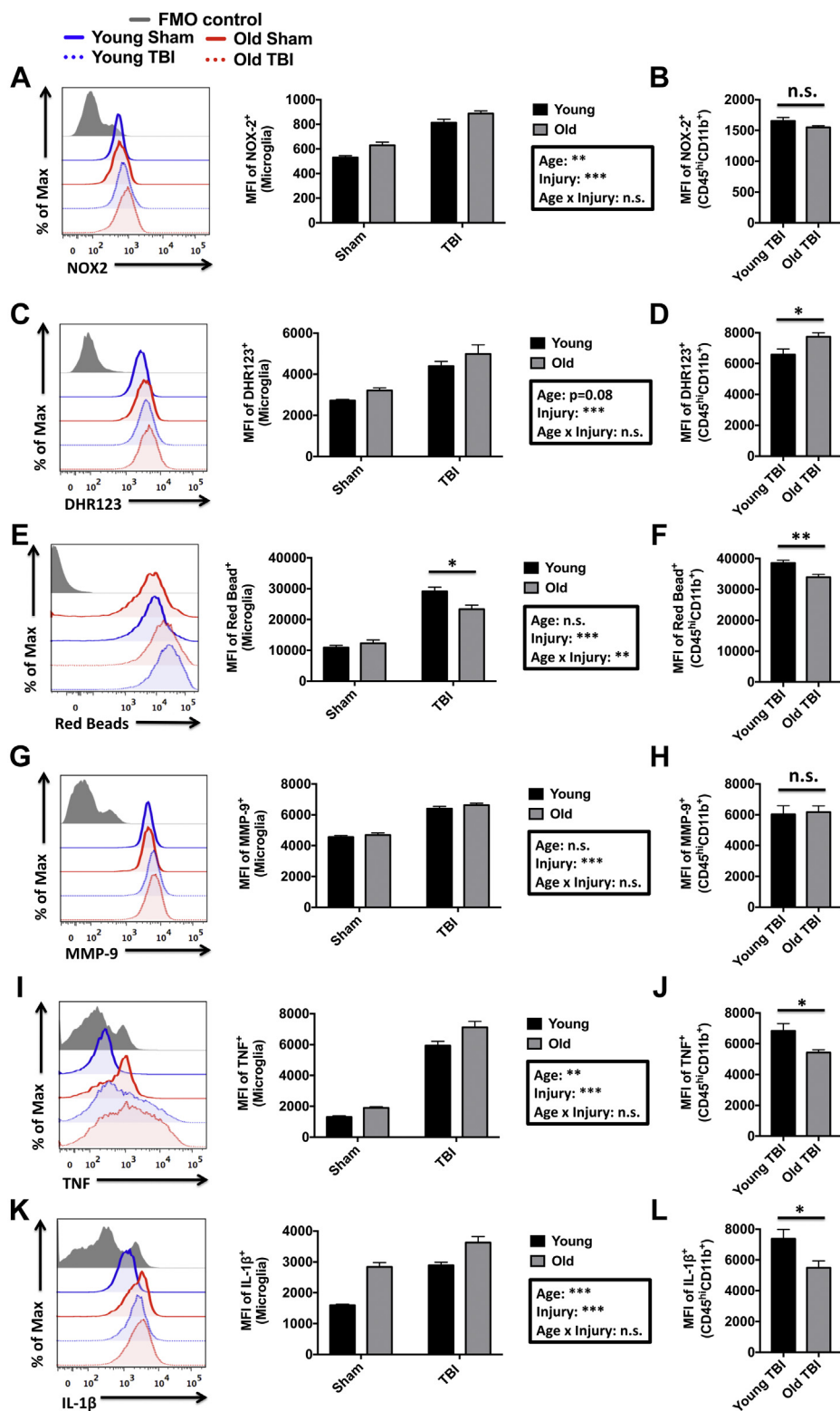


Fig. 3. Age-related changes in the functional response of microglia and infiltrating myeloid cells after acute TBI. A representative histogram depicts the relative expression level of NOX2 in brain-resident microglia (A). The MFI of NOX2-positive microglia is shown to the right, demonstrating an effect of age and injury in microglial expression. No change was seen in NOX2 MFI between young and aged CD45^{hi}CD11b⁺ infiltrating myeloid populations after TBI (B). A representative histogram shows the relative production level of reactive oxygen species, as measured by DHR123 (C). MFI quantification of DHR123-positive cells reveals a significant effect of injury on microglial-derived ROS production. A comparison of DHR123 MFI in young and old infiltrating myeloid cells is shown (D). A representative histogram illustrates the relative differences in the phagocytic uptake of fluorescent red beads in young and old microglia after TBI (E). To the right, the MFI quantification of red bead-positive microglia in young and old mice demonstrates that the relative level of phagocytosis induced by TBI is reduced in older microglia populations. The relative level of phagocytic activity in young and old infiltrating myeloid cells is shown (F). A representative histogram depicts the relative expression level of MMP-9 in brain myeloid cells (G). MFI quantification of MMP-9-positive microglia is shown for young and aged mice at 3 days after TBI. No difference in relative MMP-9 expression between young and old infiltrating myeloid populations was found (H). A representative histogram shows the relative expression level of TNF (I). MFI quantification of TNF-positive cells shows a significant increase in microglia with both injury and age. An age-related decrease in TNF production was

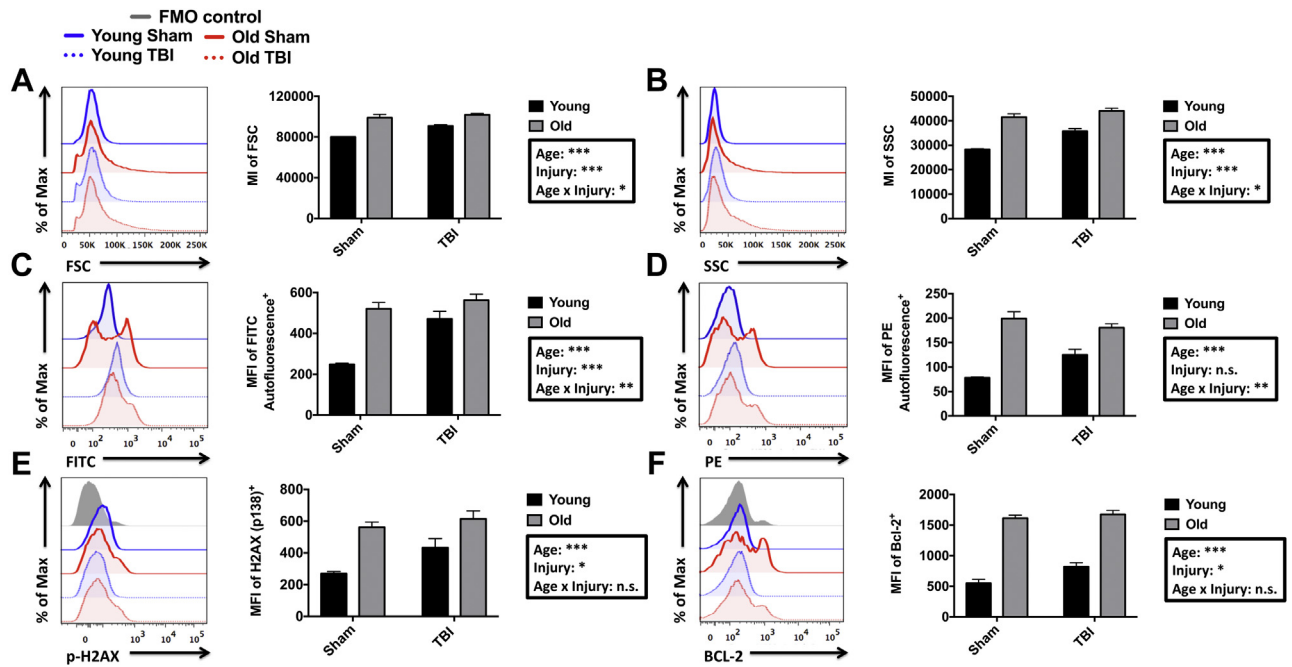


Fig. 4. Evidence of age- and TBI-induced immune senescence in the resident microglia population. A representative histogram is shown for the FSC intensity of microglia after TBI (A). MI quantification of this histogram revealed a significant effect of both age and injury, as well as a statistical interaction. A representative histogram is shown for the SSC intensity of microglia (B). To the right, MI quantification demonstrated a significant effect of both age and injury, as well as a statistical interaction. A representative histogram illustrates the relative intensity of microglial autofluorescence in the FITC channel (C). MFI quantification of these data is shown. A representative histogram shows the relative intensity of microglial autofluorescence in the PE channel (D), and MFI quantification is shown to the right. A representative histogram depicts the relative expression level of phosphorylated (Ser139) H2AX in microglia populations (E). MFI quantification of p-H2AX-positive microglia reveals a significant group effect of both age and injury. A representative histogram shows the relative expression level of BCL-2 in microglia, and the MFI quantification of BCL-2-positive microglia is shown (F). For scatter data, $N = 7$ sham and $N = 12$ TBI/group. For all other experiments, $N = 3$ sham and $N = 6$ TBI/group. Statistical comparisons between groups were determined by the two-way ANOVA with Tukey's multiple comparisons test. Significant group effects of age, injury, and interaction between age and injury are shown in each box. Error bars show mean \pm SEM. * $p < 0.05$, ** $p < 0.01$, and *** $p < 0.001$. Abbreviations: ANOVA, analysis of variance; BCL-2, B cell lymphoma 2; FMO, fluorescence minus one; FITC, fluorescein isothiocyanate; FSC, forward scatter; H2AX, histone 2a X; MI, mean intensity; MFI, mean fluorescence intensity; n.s., not significant; PE, phycoerythrin; SEM, standard error of mean; SSC, side scatter; TBI, traumatic brain injury.

determined by Western blot analysis (Fig. 5C–E). Expression of p16^{ink4a} protein, but not p21^{cip1a}, was significantly increased with normal aging. Notably, when we probed cellular senescence in microglia, we identified a significant interaction between age and TBI in the percentage of p16^{ink4a}-positive microglia, with the highest frequencies observed in aged TBI mice (Fig. 5F). The percentage of p21^{cip1a}-positive microglia was also significantly increased with age, but unaffected by TBI (Fig. 5G). Taken together, these findings demonstrate that normal aging increases the expression of senescence markers within the microglia population and more widely in the cerebral cortex, which can be differentially altered after TBI.

3.5. Aging alters TBI-induced changes in the systemic immune response

Systemic immune activation shapes brain injury outcomes and is an important predictor of TBI severity and recovery (Hazeldine et al., 2015). We explored the possibility that aging alters the systemic response to TBI. Blood and the spleen from young and aged sham and TBI mice were collected to evaluate changes in leukocyte composition and counts by flow cytometry. Blood neutrophilia is a

hallmark of acute TBI and is an indirect measure of bone marrow activation (Ritzel et al., 2018a). We found that total CD11b⁺ myeloid, Ly6C⁺ monocyte, and Ly6G⁺ neutrophil counts were similarly increased in blood from young and aged TBI mice at 72 hours after injury (Supplemental Fig. 1A). We then examined the splenic response to TBI. Spleen weights were significantly increased in young TBI mice as previously reported (Supplemental Fig. 1B) (Ritzel et al., 2018a). However, TBI-induced splenomegaly was less pronounced in aged TBI mice, and spleen mass was not significantly different between sham and injured aged mice. An analysis of leukocyte counts revealed that the increase in spleen size in young TBI mice was associated with greater accumulation of myeloid cells (Supplemental Fig. 1C). No such increase in splenic myeloid cells was observed in aged TBI mice. Collectively, these data suggest that, despite aged mice having greater behavioral deficits and an exacerbated neuroinflammatory response, the systemic response to TBI is either attenuated with age or similarly impacted.

4. Discussion

TBI is associated with increased mortality and poorer functional outcome in older patients, yet the underlying molecular and

in the infiltrating myeloid population after TBI (J). A representative histogram illustrates the relative expression level of IL-1 β (K). To the right, MFI quantification of IL-1 β -positive microglia demonstrates a significant effect of both age and injury. The relative production level of IL-1 β is shown for infiltrating myeloid populations (L). For all experiments, $N = 4$ sham and $N = 6$ TBI/group. Statistical comparisons between groups were determined by the two-way ANOVA with Tukey's multiple comparisons test. Significant group effects of age, injury, and interaction between age and injury are shown in each box. Error bars show mean \pm SEM. * $p < 0.05$, ** $p < 0.01$, and *** $p < 0.001$. Abbreviations: ANOVA, analysis of variance; DHR123, dihydrorhodamine 123; FMO, fluorescence minus one; IL-1 β , interleukin-1 beta; MFI, mean fluorescence intensity; MMP-9, matrix metalloproteinase-9; NOX2, NADPH oxidase 2; n.s., not significant; SEM, standard error of mean; TBI, traumatic brain injury; TNF, tumor necrosis factor.

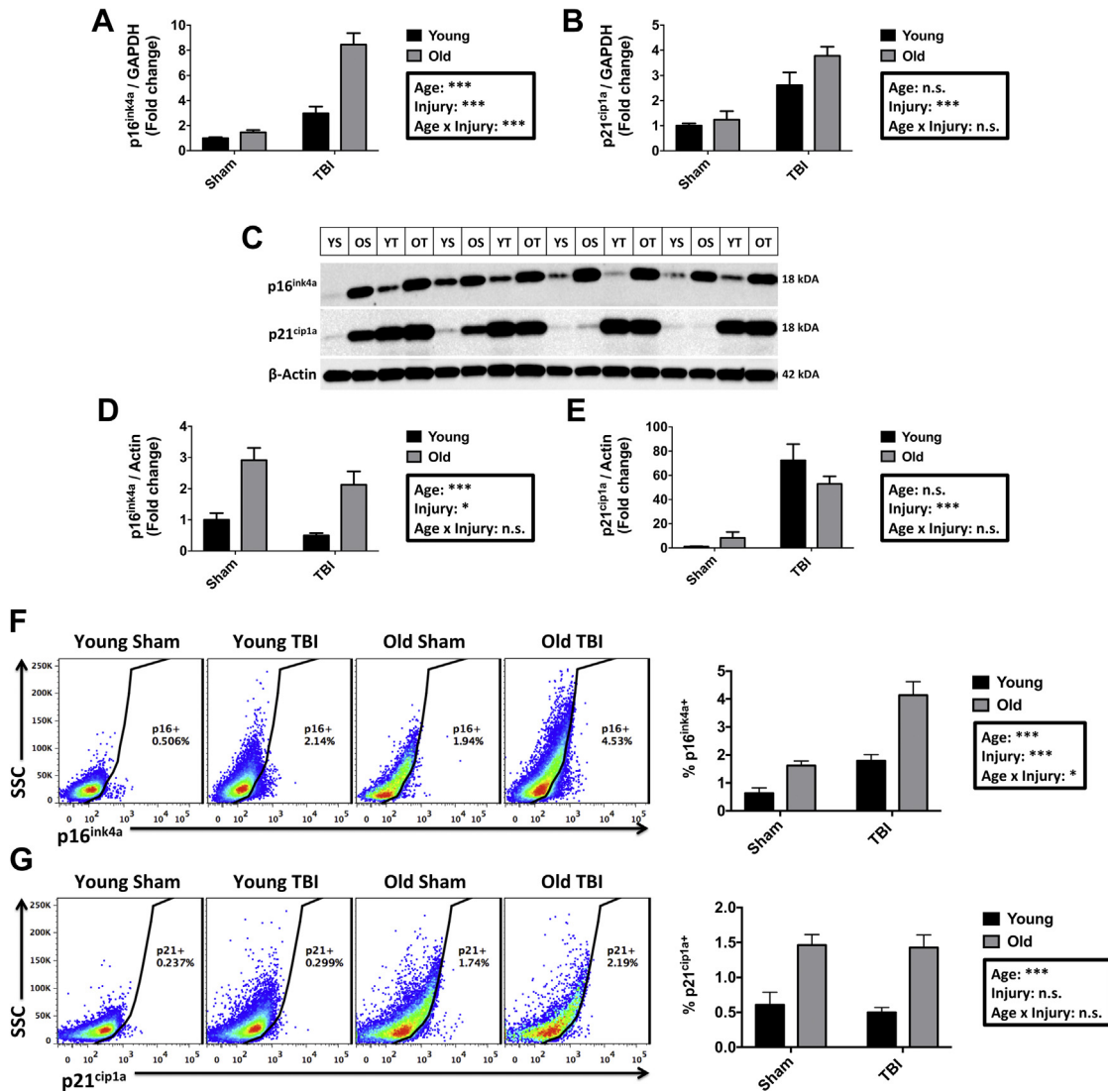


Fig. 5. Gene and protein expression of senescence markers in the aging cortex and microglia after acute TBI. Relative gene expression was determined by qPCR and expressed as fold-change to young naïve levels. A significant interaction was seen between age and injury in tissue expression of p16^{ink4a} (A). A significant effect of injury was seen in the gene expression level of p21^{cip1a} (B). Representative Western blot images are shown for p16^{ink4a}, P21^{cip1a}, and actin expression using whole cell lysate from cortical tissue of young and aged sham and TBI mice at 72 hours after injury (C). Quantification of densitometric analysis revealed an effect of both age and injury on the relative expression of p16^{ink4a} protein (D). The relative expression level of p21^{cip1a} protein was increased with injury in both groups (E). Representative dot plots show the percentage of p16^{ink4a}-positive microglia (F). Percent quantification of p16^{ink4a}-positive microglia shows a significant interaction, including a group effect of both age and injury. Representative dot plots show the percentage of p21^{cip1a}-positive microglia (G). A significant group effect of age, but not injury, was seen in the percent quantification of p21^{cip1a}-positive microglia. For all experiments, N = 4–6/group. Statistical comparisons between groups were determined by the two-way ANOVA with Tukey's multiple comparisons test. Significant group effects of age, injury, and interaction between age and injury are shown in each box. Error bars show mean ± SEM. **p* < 0.05, and ****p* < 0.001. Abbreviations: ANOVA, analysis of variance; n.s., not significant; SEM, standard error of mean; TBI, traumatic brain injury.

cellular mechanisms of secondary injury in the aged brain are poorly understood. The present study provides a comprehensive examination of how aging impacts phenotypic and functional markers of post-traumatic neuroinflammation. We demonstrate that aging increases microglial sensitivity to TBI, altering their proliferation potential, oxidative stress response, phagocytic behavior, and cytokine profile. Aging also increased the number and compositional makeup of brain-invading myeloid cells, differentially affecting their functional response to TBI. In addition, we provide the first evidence that aging increases the expression of senescence markers in the resident microglia population. These senescence markers can also be induced by TBI. We report that age-related impairments in neuroimmune function were accompanied by deficits in muscle strength, locomotor activity, endurance level, and motor coordination. Thus, our data identify several

distinguishing features of the neuroinflammatory response to TBI in the aged brain, including the functional resolution of resident and infiltrating macrophage populations, further underscoring the need for more in-depth analysis of coexisting central and systemic immune pathway dysfunction that occur in the aged brain after TBI.

Perhaps surprisingly, our flow cytometry analysis showed that the total number of hemispheric microglia were substantially lower in old mice. The reason for this decrease is unclear but appears to parallel the transition of microglia from a ramified morphology to a dystrophic state, indicating an age-related impairment in both cell turnover/repopulation and cellular resilience pathways (Streit and Xue, 2014). These findings are consistent with those from several other studies using various methods to enumerate microglia in old mice (Ritzel et al., 2018b; Sharaf et al., 2013; Sun et al., 2013; Zoller et al., 2018). A global (or region-specific) reduction in microglia

could have profound effects on CNS homeostasis. Moreover, the increased conversion of healthy microglia into dysfunctional dystrophic cells could greatly impact the brain's ability to maintain and repair itself. Aging also altered the microglial response to TBI, and microglial proliferation was significantly increased in old mice after TBI. Thus, whereas the TBI-induced proliferation potential was increased, basal homeostatic proliferation rates in microglia appeared to be inhibited or impaired. Others have demonstrated a comparable increase in the global tissue expression level of CD11b/Iba1 (Kumar et al., 2013; Sandhir et al., 2008), and our data provide confirmation at the cellular level that the increase in these myeloid-specific proteins is driven not only by the extensive influx of migrating leukocytes but also by microglial proliferation. Although these myeloid populations were clearly delineated in our flow cytometry dot plots, it is important to note that although the CD45^{int}CD11b⁺Ly6C⁻ microglia gating strategy employed in this study is extremely precise under homeostatic conditions, after TBI the gating may be altered by increased CD45 expression in activated microglia or downregulated Ly6C expression in newly resident bone marrow-derived monocytes (Greter et al., 2015). Nevertheless, most CD45^{int} and CD45^{hi} myeloid cells exhibited striking differences with age after cortical injury.

How aged microglia respond to acute brain trauma is not well understood and may vary depending on the type of injury or the disease models employed. Aging impacts many cellular processes in microglia/macrophages, with some being potentially detrimental and others being adaptive and neuroprotective (Mattson and Arumugam, 2018). Although IL-1 β induction was highly pronounced with both age and injury, suggesting an age-related increase in microglial inflammasome activity, proinflammatory cytokine production was generally decreased in peripheral myeloid populations in the aged TBI brain. Age-related changes in macrophage/macrophage polarization and transition states have been described (Kumar et al., 2013). However, peripheral macrophage reductions in TNF, IL-1 β , and MMP-9 were not associated with better outcomes and may suggest that injury severity is also driven by cytokine-independent pathways, as several studies have highlighted the importance of the dual nature of inflammation in the brain's response to injury (Chaturvedi and Kaczmarek, 2014; Clausen et al., 2016; Patel et al., 2013). We also demonstrated marked changes in other cellular immune functions that could profoundly alter outcomes, such as phagocytosis and ROS production. TBI-induced phagocytosis was blunted in aged microglia and also infiltrating populations. Given that our laboratory, and others, have demonstrated that old rodents have greater lesion volumes after TBI (Itoh et al., 2013; Kumar et al., 2013), such changes may reflect an inability to clear neuronal debris, which consequently impedes the recovery process. However, other studies have reported that the greater loss of neurological function in aged TBI mice cannot be fully explained by acute lesion size (i.e., tissue loss at the impact site) alone and demonstrate that prolonged edema and BBB disruption in aged mice underscore the importance of secondary processes in age-related TBI outcomes (Onyszchuk et al., 2008; Timaru-Kast et al., 2012). Vascular dysfunction also promotes neuroinflammation and contributes to secondary injury in TBI and chronic neurodegeneration (Erturk et al., 2016; Faden et al., 2016). Thus, our finding of phagocytic impairment could have important implications with regard to the chronic effects of TBI and may be one overlapping or contributing factor to the higher rates of amyloid plaque deposition in Alzheimer's disease or phosphorylated tau accumulation in chronic traumatic encephalopathy (Ramos-Cejudo et al., 2018; Streit and Xue, 2014). The present study is limited to the acute injury period; therefore, it remains to be seen how aging intersects with TBI to impact key microglial functions such as phagocytosis during the chronic phase of recovery. Normal

aging itself has been shown to decrease beta-amyloid uptake in microglia (Njie et al., 2012; Ritzel et al., 2015b). Although not physiological cargo, fluorescent latex beads are inert and ensure that the TBI response being measured is largely unadulterated. The 0.5- μ m latex beads used in this study are more easily ingested than larger 1.0- μ m sized beads used in previous studies and likely explain the lack of baseline change previously observed with age (Rejman et al., 2004).

Marked increases in TBI-induced ROS production were also observed in old mice, both in resident microglia and infiltrating myeloid populations. Although the compositional shift to a more neutrophilic brain response in aged mice could account for the higher level of oxidative stress, similar increases have been observed in other age-related disease and injury models, including Parkinson's and Alzheimer's diseases and stroke (Cheignon et al., 2018; Qin et al., 2013; Radak et al., 2011; Rosenzweig and Carmichael, 2013). Although global brain levels of ROS were not measured, the higher numbers of microglia and peripheral myeloid cells in the injured brains of older mice suggest that tissue levels are likely similarly higher. The consequences of higher oxidative stress levels in the brain are not just hypothetical because several studies have demonstrated that aging increases neuronal sensitivity to ROS, leading to greater cell death (Foster et al., 2008; Wang and Michaelis, 2010; Xu et al., 2007). NOX2 protein expression levels were significantly higher in the infiltrating myeloid population but did not parallel intracellular ROS production, suggesting that NOX2 activity may be differentially affected in these cells. Nonetheless, the NOX2 expression pattern largely mirrored ROS production in microglia, potentially making it a more reliable surrogate marker of ROS in these cells. Higher levels of NADPH oxidase (including NOX2) and reduced antioxidant enzyme expression were previously found in the brain of aged TBI mice, including in enriched microglia/macrophage populations (Kumar et al., 2013; Morganti et al., 2015). Thus, the present data imply that age-related elevations in microglia/myeloid-mediated oxidative stress may be a major contributor to neuronal injury in older mice.

Increased oxidative stress levels are critical for the induction and maintenance of cell senescence processes (Davalli et al., 2016). In response to chronic stress, cells can incur DNA, lipid, and protein damage as a result of increased oxidative stress (Maes et al., 2011). Exogenous and endogenous ROS can pose a significant threat to cellular integrity leading to a state of dysregulation and homeostatic dysfunction. Senescence is characterized by the induction of a secretory phenotype, increased release of inflammatory factors, and is accompanied by the errant upregulation of tumor suppressor proteins, which prevents self-targeted destruction by programmed cell death (Campisi, 2013). Aging increases cellular senescence, which has been proposed to be the cause of many age-related pathologies, including neurodegeneration. Historical studies and more recent work describing "dark microglia" have identified older microglia as having very high granular content and electron-dense cytoplasm (Bisht et al., 2016; Samorajski, 1976; Vaughan and Peters, 1974). These dark inclusions reflect a pathological state that can also be found after a TBI or during chronic neurodegeneration. In this study, we examined senescence markers in microglia and the injured cortex. Changes in the physical characteristics of microglia were detected by their unique light scatter properties on the flow cytometer (SSC and FSC). Notably, the effects of normal aging on microglial size and granularity were more pronounced than the changes induced by TBI. Although subtle increases in microglia size and granularity were detected in aged mice after TBI, there appeared to be a ceiling effect, which was not observed in young TBI mice. Because age-related granules present in non-dividing cells often indicate lipofuscin, material in the lysosomal compartment that cannot be degraded, we examined signs of autofluorescence.

With normal aging, the accumulation of lipofuscin-like material occurs in neurons and glia and may affect all aspects of cellular physiology and possibly reflect CNS pathological states (Moreno-Garcia et al., 2018). The effect of aging alone was far more profound than the effect of TBI in increasing the level of autofluorescence in the FITC or PE channels. However, the relatively greater increase in autofluorescence in young microglia after TBI was noteworthy and may reflect acute changes in lysosomal degradation or autophagy in microglia. Furthermore, it may pose an otherwise underappreciated challenge in accurately detecting changes using FITC- and PE-labeled antibodies by standard immunofluorescence microscopy and flow cytometry. Although it is not clear to what extent injury-induced autofluorescence interferes with typical immune-based fluorescence staining, it does suggest that negative controls using surgery-matched (sham-sham, TBI-TBI) tissues are needed to discern real from false-positive fluorescence signals. A recent study suggested that injury-induced microglial autofluorescence in young mice is indicative of newly phagocytosed material (i.e., CNS debris, myelin, etc.) (Greenhalgh and David, 2014), which is consistent with our findings. It is unknown whether autofluorescent microglia in young TBI mice retain this phenotype with age or if they subsequently degrade this material and return to a normal state. With age, a high proportion of rodent and human microglia exhibit a so-called dystrophic phenotype, characterized by high granularity, gnarled morphology, increased activation markers, and lipofuscin accumulation (Lopes et al., 2008; Streit et al., 2004; Wong, 2013). Senescent macrophages and microglia are also characterized by lysosomal dysfunction, which has been demonstrated to impair phagocytic clearance (Majumdar et al., 2007; Safaiyan et al., 2016). In Alzheimer's disease, balanced microglia activity contributes to amyloid-beta clearance, whereas unbalanced or dysregulated activity can result in bystander neuronal injury (ElAli and Rivest, 2016). Interestingly, in humans, degenerating neurons more closely colocalize with severely fragmented microglia than activated microglia (Streit et al., 2009). Furthermore, emerging data suggest that dystrophic microglia respond to ischemic injury in a dysregulated manner, exhibiting an exaggerated increase in ROS production and blunted TNF expression compared with their non-dystrophic counterparts (Ritzel et al., 2018b). Whether this subpopulation of cells responds to TBI in a similar fashion requires further investigation. The temporal manifestation of these cells may also be important in understanding the onset of age-related neurological decline, as some studies suggest that microglial dystrophy precedes the spread of tau-dependent neurodegeneration (Streit et al., 2009). In the present study, we used 18-month-old animals as our "old" cohort of C57Bl/6 mice. Mice have a lifespan of around 24 months, wherein "old" is defined by a minimum age of at least 18 months, at which time biomarkers of old age can be detected (Dutta and Sengupta, 2016). It is unknown how 18-month-old mice translate to human aging years, but some estimates correlate this age to 56–69 human years (Flurkey et al., 2007). Thus, while the age of the old mice used in our study may translate to a minimum of 56 human years, is it reasonable to assume that the microglial response to TBI becomes even more dysregulated with increasing age.

Cellular senescence is a well-established phenomenon that has been widely characterized *in vitro* and *in vivo*; however, senescent cells are considered rare even in aged tissues. Despite their low frequencies, senescent cells are highly dysregulated, decrease tissue function, and are resistant to apoptosis, thereby enabling them to continually produce proinflammatory factors (He and Sharpless, 2017). Furthermore, studies have demonstrated that cellular senescence is transmissible and can spread to neighboring cells via secretory molecules (Chen et al., 2018; Nelson et al., 2012). Unlike in

other tissues, relatively few studies have examined the expression of senescence markers in the brain, let alone within the resident microglial population. Thus, evidence of microglial senescence, using accepted markers, remains scarce. Our study demonstrated that normal aging increases protein expression of p16^{ink4a}, p21^{cip1a}, BCL-2, and H2AX phosphorylation in microglia. Tissue-level gene expression of p16^{ink4a} and p21^{cip1a} and protein expression of p16^{ink4a} were significantly increased in older mice. These data are consistent with other studies citing higher expression of p16^{ink4a} in the normal aged brain and in other cell types *in vivo*, including neurons, neuronal progenitors, and astrocytes (Al-Mashhadi et al., 2015; Bhat et al., 2012; Jurk et al., 2012; Krishnamurthy et al., 2004; Molofsky et al., 2006; Salminen et al., 2011). Interestingly, tau and beta-amyloid proteins have been shown to associate with and aggravate neuronal senescence in postmortem human tissue and rodent models, respectively (Musí et al., 2018; Wei et al., 2016). A quantitative reference for the stereotypical number or frequency of senescent microglia/macrophages in the aged brain is currently lacking, due in part to the complexity of defining specific criteria for glial senescence *in vivo*. Although the percentage of p16^{ink4a}-positive microglia ranged from 1% to 4% of total population in our study, this is consistent with senescent cell numbers in other tissues and reflects a significant number of dysfunctional senescent cells. Indeed, very small numbers of transplanted senescent cells are enough to cause lasting physical dysfunction (Hall et al., 2016; Xu et al., 2017, 2018). It is yet to be determined whether this microglial senescent phenotype is more prevalent in specific regions of the brain or if they are more uniformly distributed throughout the CNS. Recent reports indicate that stress and injury can induce a senescent phenotype in vulnerable cells (Chiche et al., 2017; Hornsby, 2010). Notably, the stereotypical marker of senescence, p16^{ink4a}, may be more highly expressed in long-term cultured microglia than acutely isolated microglia from normal aged mice (Stojiljkovic et al., 2019). Our data show significant TBI-induced expression of p16^{ink4a}, p21^{cip1a}, and H2AX phosphorylation in microglia, with p16^{ink4a} showing the most striking change. The discord between gene and protein level expression may reflect changes in transcriptional regulation, whereas the apparent discrepancy at the cell (i.e., microglia) and tissue level likely reflects heterogeneous expression patterns in various cell types. Given their multifunctional nature, these data highlight the need to measure senescence markers using more than one method of detection. Nevertheless, we have identified a subpopulation of microglia in the aged brain that express senescence markers. Follow-up studies are required to determine the unique functional properties of senescent microglia and how they contribute to acute and chronic brain injury.

In summary, our data show that aging alters both the peripheral immune response and microglial sensitivity to TBI, as demonstrated by changes in proliferation, extravasation, oxidative stress, phagocytosis, and cytokine production. The identification of age-related and TBI-induced microglial senescence suggests that these pathways may be viable therapeutic targets.

Disclosure

No competing financial interests exist.

Acknowledgements

The authors would like to acknowledge Nicholas Braganca, BSc, and Wesley Shoap, BSc, for their technical assistance. The authors thank Xiaoxuan Fan, PhD, and Karen Underwood, BSc, of the University of Maryland Greenebaum Comprehensive Cancer Center Flow Cytometry Facility for support with flow cytometry studies.

This work was supported by the National Institutes of Health, United States grants R01NS082308 (DJL), R01NS037313 (AIF), F32NS105355 (RMR), and T32AI095190 (SJD) and the National Institute on Aging (NIA) Claude D. Pepper Older Americans Independence Center P30-AG028747 (DJL).

Appendix A. Supplementary data

Supplementary data associated with this article can be found, in the online version, at <https://doi.org/10.1016/j.neurobiolaging.2019.02.010>.

References

- Abdul-Muneer, P.M., Chandra, N., Haorah, J., 2015. Interactions of oxidative stress and neurovascular inflammation in the pathogenesis of traumatic brain injury. *Mol. Neurobiol.* 51, 966–979.
- Al-Mashhadi, S., Simpson, J.E., Heath, P.R., Dickman, M., Forster, G., Matthews, F.E., Brayne, C., Ince, P.G., Wharton, S.B., Medical Research Council Cognitive, F., Ageing, S., 2015. Oxidative glial cell damage associated with white matter lesions in the aging human brain. *Brain Pathol.* 25, 565–574.
- Bhat, R., Crowe, E.P., Bitto, A., Moh, M., Katsetos, C.D., Garcia, F.U., Johnson, F.B., Trojanowski, J.Q., Sell, C., Torres, C., 2012. Astrocyte senescence as a component of Alzheimer's disease. *PLoS One* 7, e45069.
- Bisht, K., Sharma, K.P., Lecours, C., Sanchez, M.G., El Hajj, H., Milior, G., Olmos-Alonso, A., Gomez-Nicola, D., Luheshi, G., Vallieres, L., Branchi, I., Maggi, L., Limatola, C., Butovsky, O., Tremblay, M.E., 2016. Dark microglia: a new phenotype predominantly associated with pathological states. *Glia* 64, 826–839.
- Campisi, J., 2013. Aging, cellular senescence, and cancer. *Annu. Rev. Physiol.* 75, 685–705.
- Chaturvedi, M., Kaczmarek, L., 2014. Mmp-9 inhibition: a therapeutic strategy in ischemic stroke. *Mol. Neurobiol.* 49, 563–573.
- Cheignon, C., Tomas, M., Bonnefont-Rousselot, D., Faller, P., Hureau, C., Collin, F., 2018. Oxidative stress and the amyloid beta peptide in Alzheimer's disease. *Redox Biol.* 14, 450–464.
- Chen, N.C., Partridge, A.T., Tuzer, F., Cohen, J., Nacarelli, T., Navas-Martin, S., Sell, C., Torres, C., Martin-Garcia, J., 2018. Induction of a senescence-like phenotype in cultured human fetal microglia during HIV-1 infection. *J. Gerontol. A Biol. Sci. Med. Sci.* 73, 1187–1196.
- Chiche, A., Le Roux, I., von Joest, M., Sakai, H., Aguin, S.B., Cazin, C., Salam, R., Fiette, L., Alegria, O., Flamant, P., Tajbakhsh, S., Li, H., 2017. Injury-induced senescence enables in vivo reprogramming in skeletal muscle. *Cell Stem Cell.* 20, 407–414.e4.
- Childs, B.G., Baker, D.J., Kirkland, J.L., Campisi, J., van Deursen, J.M., 2014. Senescence and apoptosis: dueling or complementary cell fates? *EMBO Rep.* 15, 1139–1153.
- Clausen, B.H., Degn, M., Sivasaranaparan, M., Fogtmann, T., Andersen, M.G., Trojanowski, M.D., Gao, H., Hvidsten, S., Baun, C., Deierborg, T., Finsen, B., Kristensen, B.W., Bak, S.T., Meyer, M., Lee, J., Nedospasov, S.A., Brambilla, R., Lamberts, K.L., 2016. Conditional ablation of myeloid TNF increases lesion volume after experimental stroke in mice, possibly via altered ERK1/2 signaling. *Sci. Rep.* 6, 29291.
- Coronado, V.G., Thomas, K.E., Sattin, R.W., Johnson, R.L., 2005. The CDC traumatic brain injury surveillance system: characteristics of persons aged 65 years and older hospitalized with a TBI. *J. Head Trauma Rehabil.* 20, 215–228.
- Davalli, P., Mitic, T., Caporali, A., Lauriola, A., D'Arca, D., 2016. ROS, cell senescence, and novel molecular mechanisms in aging and age-related diseases. *Oxid. Med. Cell Longev.* 2016, 3565127.
- Doran, S.J., Ritzel, R.M., Glaser, E.P., Henry, R.J., Faden, A.I., Loane, D.J., 2018. Sex differences in acute neuroinflammation after experimental traumatic brain injury are mediated by infiltrating myeloid cells. *J. Neurotrauma*. [Epub ahead of print]. <http://doi.org.proxy-hs.researchport.umd.edu/10.1089/neu.2018.6019>.
- Dutta, S., Sengupta, P., 2016. Men and mice: relating their ages. *Life Sci.* 152, 244–248.
- ElAli, A., Rivest, S., 2016. Microglia in Alzheimer's disease: a multifaceted relationship. *Brain Behav. Immun.* 55, 138–150.
- Erturk, A., Mentz, S., Stout, E.E., Hedehus, M., Dominguez, S.L., Neumaier, L., Krammer, F., Llovera, F., Srinivasan, K., Hansen, D.V., Liesz, A., Scarce-Levie, K.A., Sheng, M., 2016. Interfering with the chronic immune response rescues chronic degeneration after traumatic brain injury. *J. Neurosci.* 36, 9962–9975.
- Faden, A.I., Wu, J., Stoica, B.A., Loane, D.J., 2016. Progressive inflammation-mediated neurodegeneration after traumatic brain or spinal cord injury. *Br. J. Pharmacol.* 173, 681–691.
- Filer, W., Harris, M., 2015. Falls and traumatic brain injury among older adults. *N. C. Med. J.* 76, 111–114.
- Flanagan, S.R., Hibbard, M.R., Riordan, B., Gordon, W.A., 2006. Traumatic brain injury in the elderly: diagnostic and treatment challenges. *Clin. Geriatr. Med.* 22, 449–468 x.
- Flurkey, K., Curren, J.M., Harrison, D., 2007. Mouse models in aging research. In: *The Mouse in Biomedical Research*, second ed. Elsevier, pp. 637–672.
- Foster, K.A., Margraf, R.R., Turner, D.A., 2008. NADH hyperoxidation correlates with enhanced susceptibility of aged rats to hypoxia. *Neurobiol. Aging* 29, 598–613.
- Fulop, T., Larbi, A., Dupuis, G., Le Page, A., Frost, E.H., Cohen, A.A., Witkowski, J.M., Franceschi, C., 2017. Immunosenescence and inflamm-aging as two sides of the same coin: friends or foes? *Front. Immunol.* 8, 1960.
- Gardner, R.C., Dams-O'Connor, K., Morrissey, M.R., Manley, G.T., 2018. Geriatric traumatic brain injury: epidemiology, outcomes, knowledge gaps, and future directions. *J. Neurotrauma*. [Epub ahead of print]. <http://doi.org.proxy-hs.researchport.umd.edu/10.1089/neu.2017.5371>.
- Ge, X., Cho, A., Ciol, M.A., Pettan-Brewer, C., Snyder, J., Rabinovitch, P., Ladiges, W., 2016. Grip strength is potentially an early indicator of age-related decline in mice. *Pathobiol. Aging Age Relat. Dis.* 6, 32981.
- Goldberg, E.L., Dixit, V.D., 2015. Drivers of age-related inflammation and strategies for healthspan extension. *Immunol. Rev.* 265, 63–74.
- Greenhalgh, A.D., David, S., 2014. Differences in the phagocytic response of microglia and peripheral macrophages after spinal cord injury and its effects on cell death. *J. Neurosci.* 34, 6316–6322.
- Greter, M., Lelios, I., Croxford, A.L., 2015. Microglia versus myeloid cell nomenclature during brain inflammation. *Front. Immunol.* 6, 249.
- Hall, B.M., Balan, V., Gleiberman, A.S., Strom, E., Krasnov, P., Virtuoso, L.P., Rydkina, E., Vujcic, S., Balan, K., Gitlin, I., Leonova, K., Polinsky, A., Chernova, O.B., Gudkov, A.V., 2016. Aging of mice is associated with p16(Ink4a)- and beta-galactosidase-positive macrophage accumulation that can be induced in young mice by senescent cells. *Aging (Albany NY)* 8, 1294–1315.
- Harvey, L.A., Close, J.C., 2012. Traumatic brain injury in older adults: characteristics, causes and consequences. *Injury* 43, 1821–1826.
- Hazeldine, J., Lord, J.M., Belli, A., 2015. Traumatic brain injury and peripheral immune suppression: primer and prospectus. *Front. Neurol.* 6, 235.
- He, S., Sharpless, N.E., 2017. Senescence in Health and disease. *Cell* 169, 1000–1011.
- Hernandez-Segura, A., Nehme, J., Demaria, M., 2018. Hallmarks of cellular senescence. *Trends Cell Biol.* 28, 436–453.
- Herranz, N., Gil, J., 2018. Mechanisms and functions of cellular senescence. *J. Clin. Invest.* 128, 1238–1246.
- Hornsby, P.J., 2010. Stress-Induced Senescence. In: Adams, P.D., Sedivy, J.M. (Eds.), *Cellular Senescence and Tumor Suppression*. Springer New York, New York, NY, pp. 85–106.
- Itoh, T., Imano, M., Nishida, S., Tsubaki, M., Mizuguchi, N., Hashimoto, S., Ito, A., Satou, T., 2013. Increased apoptotic neuronal cell death and cognitive impairment at early phase after traumatic brain injury in aged rats. *Brain Struct. Funct.* 218, 209–220.
- Jacotte-Simancas, A., Costa-Miserachs, D., Coll-Andreu, M., Torras-Garcia, M., Borlongan, C.V., Portell-Cortes, I., 2015. Effects of voluntary physical exercise, citicoline, and combined treatment on object recognition memory, neurogenesis, and neuroprotection after traumatic brain injury in rats. *J. Neurotrauma* 32, 739–751.
- Jurk, D., Wang, C., Miwa, S., Maddick, M., Korolchuk, V., Tzolou, A., Gonos, E.S., Thrasivoulou, C., Saffrey, M.J., Cameron, K., von Zglinicki, T., 2012. Postmitotic neurons develop a p21-dependent senescence-like phenotype driven by a DNA damage response. *Aging Cell* 11, 996–1004.
- Karibe, H., Hayashi, T., Narisawa, A., Kameyama, M., Nakagawa, A., Tominaga, T., 2017. Clinical characteristics and outcome in elderly patients with traumatic brain injury: for establishment of management strategy. *Neurol. Med. Chir. (Tokyo)* 57, 418–425.
- Krishnamurthy, J., Torrice, C., Ramsey, M.R., Kovalev, G.I., Al-Regaiey, K., Su, L., Sharpless, N.E., 2004. Ink4a/Arf expression is a biomarker of aging. *J. Clin. Invest.* 114, 1299–1307.
- Kumar, A., Stoica, B.A., Sabirzhanov, B., Burns, M.P., Faden, A.I., Loane, D.J., 2013. Traumatic brain injury in aged animals increases lesion size and chronically alters microglial/macrophage classical and alternative activation states. *Neurobiol. Aging* 34, 1397–1411.
- Loane, D.J., Pocivavsek, A., Moussa, C.E., Thompson, R., Matsuoka, Y., Faden, A.I., Rebeck, G.W., Burns, M.P., 2009. Amyloid precursor protein secretases as therapeutic targets for traumatic brain injury. *Nat. Med.* 15, 377–379.
- Lopes, K.O., Sparks, D.L., Streit, W.J., 2008. Microglial dystrophy in the aged and Alzheimer's disease brain is associated with ferritin immunoreactivity. *Glia* 56, 1048–1060.
- Maes, M., Galecki, P., Chang, Y.S., Berk, M., 2011. A review on the oxidative and nitrosative stress (O&NS) pathways in major depression and their possible contribution to the (neuro)degenerative processes in that illness. *Prog. Neuro-psychopharmacol. Biol. Psychiatry* 35, 676–692.
- Majumdar, A., Cruz, D., Asamoah, N., Buxbaum, A., Sohar, I., Lobel, P., Maxfield, F.R., 2007. Activation of microglia acidifies lysosomes and leads to degradation of Alzheimer amyloid fibrils. *Mol. Biol. Cell* 18, 1490–1496.
- Mak, C.H., Wong, S.K., Wong, G.K., Ng, S., Wang, K.K., Lam, P.K., Poon, W.S., 2012. Traumatic brain injury in the elderly: is it as bad as we think? *Curr. Transl. Geriatr. Exp. Gerontol. Rep.* 1, 171–178.
- Marin, J.R., Weaver, M.D., Mannix, R.C., 2017. Burden of USA hospital charges for traumatic brain injury. *Brain Inj.* 31, 24–31.
- Marschallinger, J., Mosher, K.I., Wyss-Coray, T., 2017. Microglial dysfunction in brain aging and neurodegeneration. In: Fulop, T., Franceschi, C., Hirokawa, K., Pawelec, G. (Eds.), *Handbook of Immunosenescence: Basic Understanding and Clinical Implications*. Springer International Publishing, Cham, pp. 1–15.
- Mattson, M.P., Arumugam, T.V., 2018. Hallmarks of brain aging: adaptive and pathological modification by metabolic states. *Cell Metabol.* 27, 1176–1199.

- Molofsky, A.V., Slutsky, S.G., Joseph, N.M., He, S., Pardal, R., Krishnamurthy, J., Sharpless, N.E., Morrison, S.J., 2006. Increasing p16INK4a expression decreases forebrain progenitors and neurogenesis during ageing. *Nature* 443, 448–452.
- Moreno-García, A., Kun, A., Calero, O., Medina, M., Calero, M., 2018. An overview of the role of lipofuscin in age-related neurodegeneration. *Front. Neurosci.* 12, 464.
- Morganti, J.M., Jopson, T.D., Liu, S., Riparip, L.K., Guandique, C.K., Gupta, N., Ferguson, A.R., Rosi, S., 2015. CCR2 antagonism alters brain macrophage polarization and ameliorates cognitive dysfunction induced by traumatic brain injury. *J. Neurosci.* 35, 748–760.
- Morganti, J.M., Riparip, L.K., Chou, A., Liu, S., Gupta, N., Rosi, S., 2016. Age exacerbates the CCR2/5-mediated neuroinflammatory response to traumatic brain injury. *J. Neuroinflammation* 13, 80.
- Musi, N., Valentine, J.M., Sickora, K.R., Baeuerle, E., Thompson, C.S., Zapata, A., Shen, Q., Orr, M.E., 2018. Tau protein aggregation induces cellular senescence in the brain. *bioRxiv* 17, e12840.
- Nelson, G., Wordsworth, J., Wang, C., Jurk, D., Lawless, C., Martin-Ruiz, C., von Zglinicki, T., 2012. A senescent cell bystander effect: senescence-induced senescence. *Aging Cell* 11, 345–349.
- Niraula, A., Sheridan, J.F., Godbout, J.P., 2017. Microglia priming with aging and stress. *Neuropsychopharmacology* 42, 318–333.
- Njie, E.G., Boelen, E., Stassen, F.R., Steinbusch, H.W., Borchelt, D.R., Streit, W.J., 2012. Ex vivo cultures of microglia from young and aged rodent brain reveal age-related changes in microglial function. *Neurobiol. Aging* 33, 195.e1–195.e12.
- Onyszczuk, G., He, Y.Y., Berman, N.E., Brooks, W.M., 2008. Detrimental effects of aging on outcome from traumatic brain injury: a behavioral, magnetic resonance imaging, and histological study in mice. *J. Neurotrauma* 25, 153–171.
- Papa, L., Mendes, M.E., Braga, C.F., 2012. Mild traumatic brain injury among the geriatric population. *Curr. Transl. Geriatr. Exp. Gerontol. Rep.* 1, 135–142.
- Patel, A.R., Ritzel, R., McCullough, L.D., Liu, F., 2013. Microglia and ischemic stroke: a double-edged sword. *Int. J. Physiol. Pathophysiol. Pharmacol.* 5, 73–90.
- Prattichizzo, F., Bonafe, M., Olivieri, F., Franceschi, C., 2016. Senescence associated macrophages and “macroph-aging”: are they pieces of the same puzzle? *Aging (Albany NY)* 8, 3159–3160.
- Qin, L., Liu, Y., Hong, J.S., Crews, F.T., 2013. NADPH oxidase and aging drive microglial activation, oxidative stress, and dopaminergic neurodegeneration following systemic LPS administration. *Glia* 61, 855–868.
- Radak, Z., Zhao, Z., Goto, S., Koltai, E., 2011. Age-associated neurodegeneration and oxidative damage to lipids, proteins and DNA. *Mol. Aspects Med.* 32, 305–315.
- Ramos-Cejudo, J., Wisniewski, T., Marmar, C., Zetterberg, H., Blennow, K., de Leon, M.J., Fossati, S., 2018. Traumatic brain injury and Alzheimer's disease: the cerebrovascular link. *EBioMedicine* 28, 21–30.
- Rejman, J., Oberle, V., Zuhorn, I.S., Hoekstra, D., 2004. Size-dependent internalization of particles via the pathways of clathrin- and caveolae-mediated endocytosis. *Biochem. J.* 377 (Pt 1), 159–169.
- Ritzel, R.M., Patel, A.R., Grenier, J.M., Crapser, J., Verma, R., Jellison, E.R., McCullough, L.D., 2015a. Functional differences between microglia and monocytes after ischemic stroke. *J. Neuroinflammation* 12, 106.
- Ritzel, R.M., Patel, A.R., Pan, S., Crapser, J., Hammond, M., Jellison, E., McCullough, L.D., 2015b. Age- and location-related changes in microglial function. *Neurobiol. Aging* 36, 2153–2163.
- Ritzel, R.M., Doran, S.J., Barrett, J.P., Henry, R.J., Ma, E.L., Faden, A.I., Loane, D.J., 2018a. Chronic alterations in systemic immune function after traumatic brain injury. *J. Neurotrauma* 35, 1419–1436.
- Ritzel, R.M., Lai, Y.J., Crapser, J.D., Patel, A.R., Schreengost, A., Grenier, J.M., Mancini, N.S., Patrizzi, A., Jellison, E.R., Morales-Scheihing, D., Venna, V.R., Kofler, J.K., Liu, F., Verma, R., McCullough, L.D., 2018b. Aging alters the immunological response to ischemic stroke. *Acta Neuropathol.* 136, 89–110.
- Rogakou, E.P., Pilch, D.R., Orr, A.H., Ivanova, V.S., Bonner, W.M., 1998. DNA double-stranded breaks induce histone H2AX phosphorylation on serine 139. *J. Biol. Chem.* 273, 5858–5868.
- Rosenzweig, S., Carmichael, S.T., 2013. Age-dependent exacerbation of white matter stroke outcomes: a role for oxidative damage and inflammatory mediators. *Stroke* 44, 2579–2586.
- Safaiyan, S., Kannaiyan, N., Snaidero, N., Brioschi, S., Biber, K., Yona, S., Edinger, A.L., Jung, S., Rossner, M.J., Simons, M., 2016. Age-related myelin degradation burdens the clearance function of microglia during aging. *Nat. Neurosci.* 19, 995–998.
- Salminen, A., Ojala, J., Kaarniranta, K., Haapasalo, A., Hiltunen, M., Soininen, H., 2011. Astrocytes in the aging brain express characteristics of senescence-associated secretory phenotype. *Eur. J. Neurosci.* 34, 3–11.
- Samorajski, T., 1976. How the human brain responds to aging. *J. Am. Geriatr. Soc.* 24, 4–11.
- Sandhir, R., Onyszczuk, G., Berman, N.E., 2008. Exacerbated glial response in the aged mouse hippocampus following controlled cortical impact injury. *Exp. Neurol.* 213, 372–380.
- Sharaf, A., Kriegelstein, K., Spittau, B., 2013. Distribution of microglia in the postnatal murine nigrostriatal system. *Cell Tissue Res.* 351, 373–382.
- Shoji, H., Takao, K., Hattori, S., Miyakawa, T., 2016. Age-related changes in behavior in C57BL/6J mice from young adulthood to middle age. *Mol. Brain* 9, 11.
- Simon, D.W., McGeachy, M.J., Bayir, H., Clark, R.S., Loane, D.J., Kochanek, P.M., 2017. The far-reaching scope of neuroinflammation after traumatic brain injury. *Nat. Rev. Neurol.* 13, 171–191.
- Stojiljkovic, M.R., Ain, Q., Bondeva, T., Heller, R., Schmeer, C., Witte, O.W., 2019. Phenotypic and functional differences between senescent and aged murine microglia. *Neurobiol. Aging* 74, 56–69.
- Streit, W.J., Xue, Q.S., 2014. Human CNS immune senescence and neurodegeneration. *Curr. Opin. Immunol.* 29, 93–96.
- Streit, W.J., Sammons, N.W., Kuhns, A.J., Sparks, D.L., 2004. Dystrophic microglia in the aging human brain. *Glia* 45, 208–212.
- Streit, W.J., Braak, H., Xue, Q.S., Bechmann, I., 2009. Dystrophic (senescent) rather than activated microglial cells are associated with tau pathology and likely precede neurodegeneration in Alzheimer's disease. *Acta Neuropathol.* 118, 475–485.
- Sun, D., McGinn, M., Hankins, J.E., Mays, K.M., Rolfe, A., Colello, R.J., 2013. Aging- and injury-related differential apoptotic response in the dentate gyrus of the hippocampus in rats following brain trauma. *Front. Aging Neurosci.* 5, 95.
- Susman, M., DiRusso, S.M., Sullivan, T., Risucci, D., Nealon, P., Cuff, S., Haider, A., Benzil, D., 2002. Traumatic brain injury in the elderly: increased mortality and worse functional outcome at discharge despite lower injury severity. *J. Trauma* 53, 219–223 discussion 23–4.
- Thompson, H.J., McCormick, W.C., Kagan, S.H., 2006. Traumatic brain injury in older adults: epidemiology, outcomes, and future implications. *J. Am. Geriatr. Soc.* 54, 1590–1595.
- Timaru-Kast, R., Luh, C., Gotthardt, P., Huang, C., Schafer, M.K., Engelhard, K., Thal, S.C., 2012. Influence of age on brain edema formation, secondary brain damage and inflammatory response after brain trauma in mice. *PLoS One* 7, e43829.
- Vaughan, D.W., Peters, A., 1974. Neuroglial cells in the cerebral cortex of rats from young adulthood to old age: an electron microscope study. *J. Neurocytol.* 3, 405–429.
- Venna, V.R., Weston, G., Benashski, S.E., Tarabishy, S., Liu, F., Li, J., Conti, L.H., McCullough, L.D., 2012. NF-kappaB contributes to the detrimental effects of social isolation after experimental stroke. *Acta Neuropathol.* 124, 425–438.
- von Bernhardi, R., Eugenin-von Bernhardi, L., Eugenin, J., 2015. Microglial cell dysregulation in brain aging and neurodegeneration. *Front. Aging Neurosci.* 7, 124.
- Wan, X., Liu, S., Wang, S., Zhang, S., Yang, H., Ou, Y., Zhao, M., James, L., Shu, K., Chen, J., Lei, T., 2016. Elderly patients with severe traumatic brain injury could benefit from surgical treatment. *World Neurosurg.* 89, 147–152.
- Wang, X., Michaelis, E.K., 2010. Selective neuronal vulnerability to oxidative stress in the brain. *Front. Aging Neurosci.* 2, 12.
- Wei, Z., Chen, X.C., Song, Y., Pan, X.D., Dai, X.M., Zhang, J., Cui, X.L., Wu, X.L., Zhu, Y.G., 2016. Amyloid beta protein aggravates neuronal senescence and cognitive deficits in 5XFAD mouse model of Alzheimer's disease. *Chin. Med. J. (Engl)* 129, 1835–1844.
- Wong, W.T., 2013. Microglial aging in the healthy CNS: phenotypes, drivers, and rejuvenation. *Front. Cell. Neurosci.* 7, 22.
- Xu, K., Sun, X., Puchowicz, M.A., LaManna, J.C., 2007. Increased sensitivity to transient global ischemia in aging rat brain. *Adv. Exp. Med. Biol.* 599, 199–206.
- Xu, M., Bradley, E.W., Weivoda, M.M., Hwang, S.M., Pirtskhalava, T., Deckleaver, T., Curran, G.L., Ogrodnik, M., Jurk, D., Johnson, K.O., Lowe, V., Tchkonja, T., Westendorf, J.J., Kirkland, J.L., 2017. Transplanted senescent cells induce an osteoarthritis-like condition in mice. *J. Gerontol. A Biol. Sci. Med. Sci.* 72, 780–785.
- Xu, M., Pirtskhalava, T., Farr, J.N., Weigand, B.M., Palmer, A.K., Weivoda, M.M., Inman, C.L., Ogrodnik, M.B., Hachfeld, C.M., Fraser, D.G., Onken, J.L., Johnson, K.O., Verzosa, G.C., Langhi, L.G.P., Weigl, M., Giorgadze, N., LeBrasseur, N.K., Miller, J.D., Jurk, D., Singh, R.J., Allison, D.B., Ejima, K., Hubbard, G.B., Ikeno, Y., Cubro, H., Garovic, V.D., Hou, X., Weroha, S.J., Robbins, P.D., Niedernhofer, L.J., Khosla, S., Tchkonja, T., Kirkland, J.L., 2018. Senolytics improve physical function and increase lifespan in old age. *Nat. Med.* 24, 1246–1256.
- Zhang, S., Kojic, L., Tsang, M., Grewal, P., Liu, J., Namjoshi, D., Wellington, C.L., Tetzlaff, W., Cynader, M.S., Jia, W., 2016. Distinct roles for metalloproteinases during traumatic brain injury. *Neurochem. Int.* 96, 46–55.
- Zhao, Z., Loane, D.J., Murray 2nd, M.G., Stoica, B.A., Faden, A.I., 2012. Comparing the predictive value of multiple cognitive, affective, and motor tasks after rodent traumatic brain injury. *J. Neurotrauma* 29, 2475–2489.
- Zoller, T., Attaai, A., Potru, P.S., Russ, T., Spittau, B., 2018. Aged mouse cortical microglia display an activation profile suggesting immunotolerogenic functions. *Int. J. Mol. Sci.* 19, 706.